

An Improved Method for Discrimination of Cell Populations in Tissue Sections Using Microscopy-Based Multicolor Tissue Cytometry

Rupert C. Ecker,^{1*} Radu Rogojanu,² Marc Streit,² Katja Oesterreicher,³ and Georg E. Steiner^{1,3}

¹TissueGnostics GmbH, Vienna, Austria

²Institute for Computer Graphics and Visualization, Technical University Graz

³Department of Urology, Medical University of Vienna, Austria

Received 18 March 2005; Revision Received 30 March 2005; Accepted 30 March 2005

Background: In tissue context, researchers and pathologists lack a generally applicable standard for quantitative determination of cytological parameters. Increasing knowledge of disease-specific markers calls for an appropriate *in situ* tissue cytometry.

Methods: Microscopy-based multicolor tissue cytometry (MMTC) permits multicolor analysis of single cells within tissue context.

Results: Tissue specimens stained for CD45/CD3/CD4/CD8 were analyzed. Specificity as well as reproducibility of MMTC is demonstrated and a novel MMTC-based func-

tion to improve visual discrimination of subpopulations is introduced.

Conclusions: Our data demonstrate that MMTC constitutes an important step toward automated and quantitative fluorometry of solid tissues and cell monolayers.

© 2006 International Society for Analytical Cytology

Key terms: microscopy-based multicolor tissue cytometry; quantitative microscopy; multicolor immunofluorescence; fluorometry; phenotypic characterization

Multicolor flow cytometry (FACS) of leukocytes represents a well established technique (1). Although image cytometry has a long history (2), no standard for quantification of immunohistologic samples, which can analyze any kind of cells in tissue, has been established so far.

The basic challenge in image cytometry is segmentation and object recognition. Microscopy-based multicolor tissue cytometry (MMTC) represents a technique to quantify tissues at the single-cell level. We applied advanced search algorithms to identify and reconstruct individual leukocytes and/or other types of cells. The methodology used throughout this article represents a microscopic equivalent to FACS (3) by allowing automated processing of multicolor-labeled tissue samples. Individual cells are identified by analyzing staining patterns and gray-value distribution, and the software measures the mean relative fluorescence per identified cell. However, a major issue associated with image cytometry at high-optical magnification was that the difference between positive and negative cell populations was much less pronounced when compared with flow cytometry. The reason is that fluorescence mean relative intensity is calculated as the mean intensity of the entire area of an object. Large objects (cells) caused by a high magnification show inhomogeneous antigen distribution for many molecular markers,

with distribution over cellular compartments (nucleus, cytoplasm) or the entire cell. The arithmetic mean value of all pixels belonging to a single cell is, therefore, considerably lowered by unstained portions.

We used improved search algorithms in the image analysis software and introduced a mathematical approach to provide reliable differentiation of subpopulations based on multiparameter immunohistology without the necessity to manipulate raw data. The respective function is “sensitivity adaptation,” an approach that facilitates the ability to discriminate positive/negative cells with respect to control staining. This transformation effects only the graphical visualization (dot-plots), rather than the original data sets, and facilitates defining cut-off values. The relationship between bound probe and measured fluorescence integrity per cell remains unchanged.

Part of this work was presented at the 10th Leipziger Workshop “Systems Biology and Clinical Cytomics,” April 7–9, 2005, Leipzig, Germany

*Correspondence to: Dr. Rupert Ecker, TissueGnostics GmbH, Taborstrasse 10/2/8, 1020 Vienna, Austria.

E-mail: rupert.ecker@tissuegnostics.com

Published online 14 February 2006 in Wiley InterScience (www.interscience.wiley.com).

DOI: 10.1002/cyto.20219

The two major problems, which may arise in this respect, are the interassay variance of the experimental system and the interspecimen variance in tissue sections. Both were determined using a staining protocol with four directly labeled monoclonal antibodies directed against CD3, CD4, CD8, and CD45 in specimens of rejected renal allografts. Moreover, MMTC was compared to FACS using peripheral blood leukocytes (PBLs).

MATERIALS AND METHODS

Tissue Collection and Fixation

Renal tissue specimens of patients undergoing transplant nephrectomy (Tx, $n = 5$) were snap-frozen in liquid nitrogen immediately after surgery and stored at -70°C . Thick sections of $5\ \mu\text{m}$ mounted on poly-L-lysine (Sigma, St. Louis, MO) coated slides were fixed in acetone for 20 min at -20°C .

Staining Procedure

After an equilibration step (at least 2 h at 4°C) with 1% bovine serum albumin (BSA, Sigma, St. Louis, MO) in 0.0067 M phosphate-buffered saline (PBS, Bio Whittaker, Verviers, Belgium), sections were blocked with 5% fat-free milk-powder in PBS-BSA for 30 min at room temperature. The fluorochromes fluorescein-isothiocyanate (FITC, $\lambda_{\text{EX}} = 488\ \text{nm}$), phycoerythrin (PE, $\lambda_{\text{EX}} = 488\ \text{nm}$), energy-coupled-dye (ECD, $\lambda_{\text{EX}} = 488\ \text{nm}$)--a tandem dye consisting of PE and TexasRed--and allophycocyanin (APC, $\lambda_{\text{EX}} = 633\ \text{nm}$) were used. Using PE-cyanin 5 (PC5, $\lambda_{\text{EX}} = 488\ \text{nm}$), instead of APC, would have allowed a single laser excitation. However, as PC5 changes its spectral property under UV-radiation (e.g., when the sample is examined visually) in a dose-dependent manner, resulting in a shift of the PC5 emission spectrum from the Cy5-domain into the PE-domain (unpublished data)--which obviously constitutes a severe problem in any spectral imaging approach--APC was used instead.

Rejected renal transplant specimens ($n = 5$) were incubated over night at 4°C , using directly labeled antibodies anti-CD45-ECD, -CD3-FITC, -CD4-PE, and -CD8-APC (Beckman Coulter, San Jose, CA), washed extensively, and cover-slipped in Geltol Aqueous Mounting Medium (Lipshaw Immunon, Pittsburg, PA). Staining specificity was controlled by isotype-matched *negative controls* in all possible combinations. Each experiment was repeated at least three times.

For the analysis of peripheral blood leukocytes by flow cytometry, PBLs were derived from human volunteers, isolated by gradient centrifugation, and stained for CD3-FITC, CD4-PE, and CD8-PC5. PBLs were analyzed by means of flow cytometry, using a FACScan (Becton Dickinson, San Jose, CA). In these experiments, PC5 had to be used, instead of APC, as the FACScan was not equipped with a 633 nm laser. To prevent UV-induced spectral shifting of PC5 in LSM, the automatic acquisition mode of TissueQuest was used to avoid UV-excitation of PC5. For comparison, PBLs from identical preparations were mounted to slides and analyzed by MMTC.

Four-Color Immunofluorescence Confocal Laser Scanning Microscopy

It has been demonstrated before that spectral imaging is superior to classical band-pass (BP) filter-based detection (4). Therefore, we used a Zeiss Laser Scanning Microscopes (LSM) 510 META (Zeiss, Jena, Germany) as centerpiece of our MMTC instrumentation. The instrument was equipped with two lasers (488 nm argon-laser and 633 nm He/Ne-laser), two photomultiplier tubes (PMT), and the META detector for spectral imaging. FITC, PE, and ECD were acquired by 488 nm excitation using the Lambda-mode. Lambda-stacks were subsequently unmixed using linear unmixing. APC was excited with the 633 nm line and recorded as single track. As FITC, PE, and ECD cannot be excited with the 633 nm laser, there was no need to unmix APC from the other three dyes. Images were recorded using a $63\times$ objective lens, and excitation intensity was kept as low as possible to avoid autofluorescence (5,6). The primary beam splitter (BS1) was a trichroic beam splitter (TBS) 488/543/633.

Image-Analysis

The principle of the method has been demonstrated elsewhere (3,7). In brief, the analysis software TissueQuest (TissueGnostics GmbH, Vienna, Austria) offers several algorithms for single-cell identification. In the current approach, the advanced leukocyte detection method was engaged (7). As the setting of segmentation parameters is crucial for analysis outcome, the algorithms are predefined and allow only minimal user manipulation. In the so-called master-channel, all measure events (=single cells) are identified. This mask is then used in a corrected form to measure staining intensity in all four channels, which is in similarity to flow cytometry. By engaging negative controls, cutoff values can be defined and the percentages of positive/negative populations are computed. In similarity to flow cytometry, these cutoff values are set in a way that some 1% of cells in the control are referred to as positive. It is only the comparison of the mean relative intensity (mean gray value) of a particular object to an appropriate negative control that allows to determine the level of specificity. The mean relative intensity is normalized for the instrument's detector sensitivity as described previously (3). Therefore, results obtained at different PMT voltage can be directly compared. Coexpressions are depicted in scattergrams (dot-plots) of normalized gray values. This detector sensitivity-normalization may result in final gray values higher than 255 (8 bit).

RESULTS

System Accuracy of MMTC/TissueQuest

To test the advanced leukocyte identification strategy and to demonstrate accuracy of MMTC, we compared the obtained results to flow cytometry (FACS) using PBL stained for anti-CD3/-CD4/-CD8.

Although basically similar, the measuring apparatus in flow cytometry and confocal laser scanning microscopy is different. While in each technique measured intensities

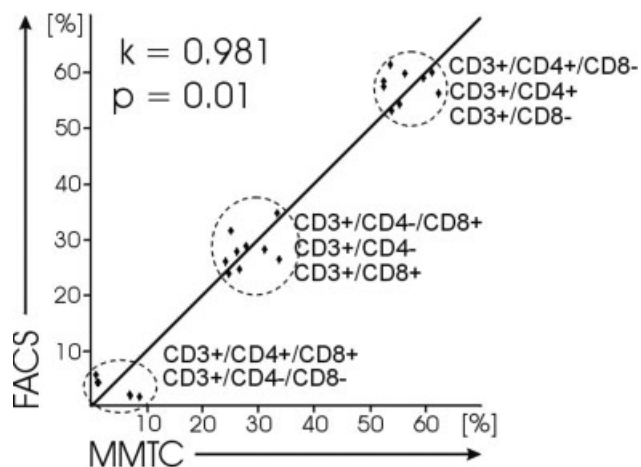


Fig. 1. Comparison of MMTC with FACS. PBLs were obtained from three different volunteers, triple stained using anti-CD3, -CD4, and -CD8 and comparatively analyzed by MMTC and FACS. In both methods, identical samples were analyzed. Isotype-matched negative controls were used to set the cut-off values for computation of positive and negative populations. The percentage of each population within the CD3⁺-subset (e.g., CD3⁺/CD4⁻/CD8⁺) was determined independently with both methods but on identical samples. The values on each axis represent the percentage of measured coreactivity of a particular marker combination obtained by MMTC versus FACS, i.e., the composition of phenotypic subpopulations. There was an excellent correlation with $k = 0.981$ after Pearson at a high confidence level of significance with $P = 0.01$. The visible clusters define certain leukocytic subpopulations among tissue infiltrating leukocytes.

are important for comparison of different samples, the intensity values of both systems are not directly comparable with each other. Therefore, we can only compare the resulting percentages calculated in careful definition of cutoff values. Results obtained by MMTC revealed a highly significant correlation to FACS (Fig. 1).

To test the reproducibility in tissue sections, experiments were repeated six times applying four color immunofluorescence on serial sections. Sections were processed in independent experiments, and the results were compared (i.e., interassay variability was determined). The data from these consecutive sections were compared with those of statistically distributed sections derived from different specimen layers of the same patient. These distributed sections were processed simultaneously in each experiment (i.e., interspecimen variability was determined). While the interassay variability was $(5.2 \pm 8.5)\%$, the interspecimen variability was almost twice as high $(9.4 \pm 13.7)\%$.

Single-Cell Identification and Image Cytometry

Anti-CD45 was used to identify tissue infiltrating leukocytes (Figs. 2a-2c). From each specimen, 30 images (enclosing a total area of 1.2384 mm^2 per specimen), which spread over the entire section, were analyzed. All of the Tx specimens contained clustered leukocytes in most of the images recorded and were, therefore, of special interest for evaluation of the actual quality of the identification strategy used.

Nonspecific mouse IgG1-ECD was used to set sensitivity for CD45-ECD. Corresponding isotype-matched controls for the other three antibodies were used to determine accurately the cutoff values for each fluorescence signal.

Enhancing Analysis Specificity by Sensitivity Adaptation

The frequently occurring problem of low relative intensity values constitutes a major issue in mean intensity-based image cytometry. In flow cytometry, a single cell is considered as point source of total fluorescence and intensity of this object is not divided among up to hundreds of image pixels. In contrast, in microscopy, single cells are an area consisting of many potential point sources of fluorescence, and the fluorometric relative intensity is calculated as the arithmetic mean of the values of all pixels. Since most antigens are not homogeneously distributed among the cell, there is considerable amount of "unstained area" within a stained object. It is true that this reflects the actual subcellular antigen distribution, but it also reduces the measured relative intensity values, a fact unconsidered in flow cytometry.

To overcome these circumstantial limitations we introduced a function called *sensitivity adaptation*. It is capable of performing a mathematical discrimination of "positive" and "negative" values based on appropriate negative controls (Fig. 3). While it was often difficult to set an appropriate cut-off in order to separate positive/negative populations on unprocessed scattergrams (Figs. 3a-3c), the sensitivity adaptation procedure facilitated their optical distinction by an algorithm that allows the user to set gain and shift values (Figs. 3d-3f). These gain- and offset-values were set at the negative controls, and identical settings were applied to all other staining combinations, which the particular negative control was valid for.

This procedure is a tool of visualization, especially of small differences, and allows an easier setting of cutoff values for calculation of statistics while fluorometry (i.e., calculation of mean intensities) is done using unmodified values, thereby improving the accuracy of the methodology.

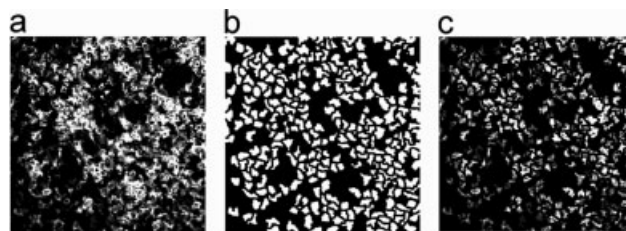


Fig. 2. Single-cell recognition by TissueQuest analysis software. Using the fluorescence signal of a dye, the search algorithm tries to reconstruct objects that resemble individual cells at the highest possible probability. (a) The anti-CD45 reactivity in a tissue section of a Tx specimen is used to (b) identify all tissue infiltrating leukocytes, and (c) the combination of a and b shows the result of the identification process in the original image.

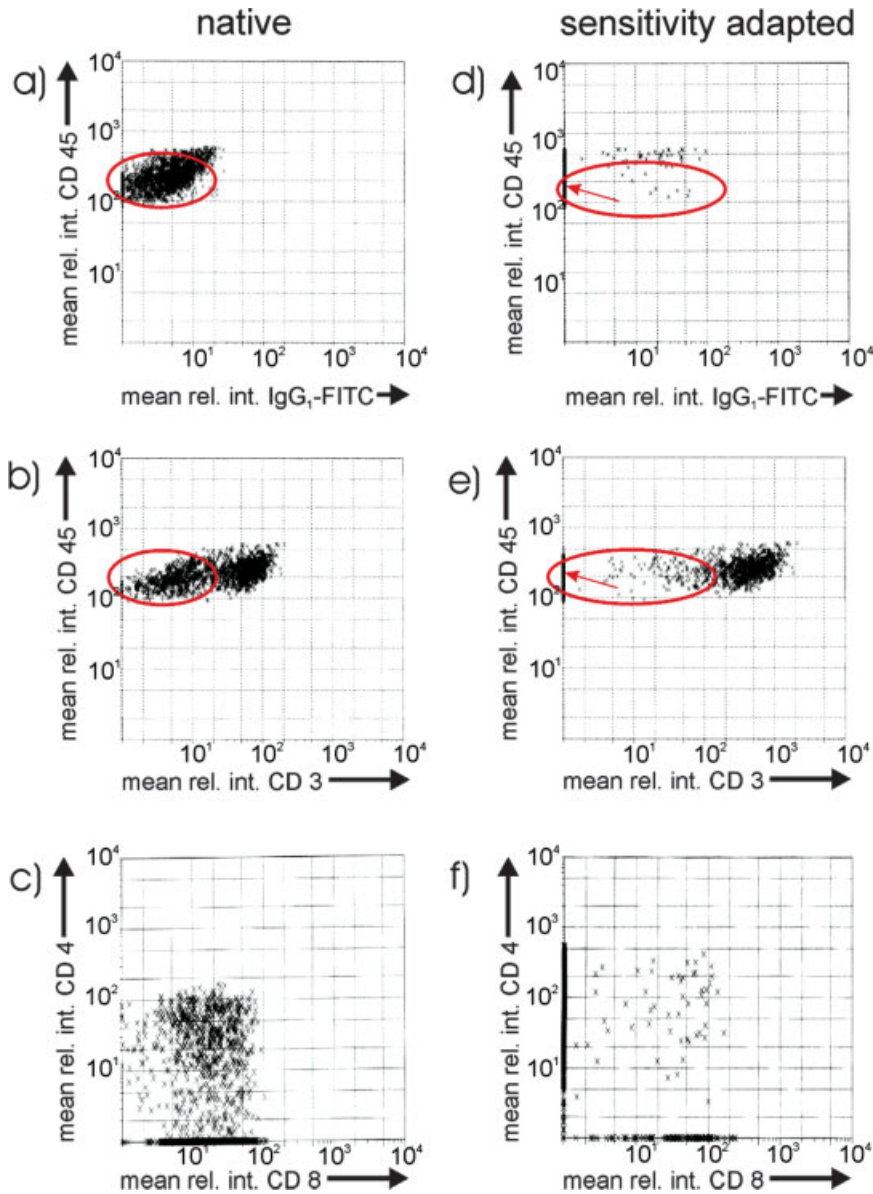


FIG. 3. Enhanced discrimination of specifically stained cell populations from background noise by sensitivity adaptation. Scattergrams shows the mean relative intensity of all measured cells. (a) Native isotype-matched negative control for native CD3-reactivity of CD45⁺ leukocytes (b); (c) CD4/CD8-reactivity of CD45⁺/CD3⁺ T-lymphocytes (d) through (f) are the identical yet sensitivity adapted cell populations. The marked areas indicate the range of the negative population in both the native and the sensitivity adapted scattergrams. As low-intensity and high-intensity events are mathematically separated, the negative population in the sensitivity adapted scattergrams gets lined up at the y-axis (x-value is zero; arrows in the lower panels). Only those cells in the negative/control population with highest gray value retain a gray value higher than zero in the adapted test data set. The test data sets are recomputed in identical manner thereby accentuating given differences without changing the measurement result. It is important to note that mean values of entire populations are calculated using unmodified (i.e., native) data sets as they are measured by fluorometry. [Color figure can be viewed in the online issue, which is available at www.interscience.wiley.com.]

DISCUSSION AND CONCLUSION

In image cytometry, there are two fundamental approaches: a-priori and a-posteriori discrimination. In a-priori approaches, relevant parameters and their thresholds are first defined by structural means, and events are measured subsequently. Measure events are defined by image objects based on parameter thresholds (3,8). In a-posteriori approaches, a set of parameters is selected, and events are measured—where at the time of measurement it is not defined which of those parameters are relevant for analysis—and relevant parameters and respective thresholds are defined subsequently by statistical means. Measure events are defined by regular image areas based on statistical thresholds (9).

The challenge with a-priori discrimination lies in appropriately segmenting the images. However, if this is achieved, the results refer directly to cell objects. While a-posteriori approaches, which need not take care about appropriate object segmentation, but search for relevant discriminators, can be successfully applied to image classification, they are not appropriate for single-cell identification in cytomics (4,10). As cytomics is a cell-based approach, only a-priori image discrimination is appropriate for use in the Human Cytochrome Project (11,12).

MMTC represents an a-priori approach and identifies single cells within tissue context. Our study further showed that a novel tool of the TissueQuest analysis software, called sensitivity adaptation, permits improved discrimination of cell subpopulations compared to native data sets. This methodology does not impose any restric-

tions on image cytometry, but facilitates visual discrimination of subpopulations and improves the accuracy when setting cut-off values for statistical analysis.

MMTC appears to be irreplaceable for linking phenotypic properties to cellular environments, hence for reliably defining an *in situ* status. This methodology constitutes an important step toward automated histopathology and computer aided molecular diagnostics.

LITERATURE CITED

1. Beavis AJ, Pennline KJ. Simultaneous measurement of five-cell surface antigens by five-colour immunofluorescence. *Cytometry* 1994;15: 371-376.
2. Goerttler K, Stohr M. Automated cytology. The state of the art. *Arch Pathol Lab Med* 1982;106:657-661.
3. Steiner GE, Ecker RC, Kramer G, Stockenhuber F, Marberger MJ. Automated data acquisition by confocal laser scanning microscopy and image analysis of triple stained immunofluorescent leukocytes in tissue. *J Immunol Methods* 2000;237:39-50.
4. Ecker RC, de Martin R, Steiner GE, Schmid JA. Application of spectral imaging microscopy in cytomics and fluorescence resonance energy transfer microscopy (FRET) microscopy. *Cytometry Part A* 2004;59A: 172-181.
5. Wahlby C, Lindblad J, Vondrus M, Bengtsson E, Bjorkesten L. Algorithms for cytoplasm segmentation of fluorescence labeled cells. *Anal Cell Pathol* 2002;24:101-111.
6. Tsien R, Waggoner A. Fluorophores for confocal microscopy. In: Pawley J, editor. *Handbook of Biological Confocal Microscopy*. New York: Plenum Press; 1995. p 267-279.
7. Ecker RC, Steiner GE. Microscopy-based multicolor tissue cytometry at the single-cell level. *Cytometry Part A* 2004;59A:182-190.
8. Gerstner AO, Trumpfheller C, Racz P, Osmancik P, Tenner-Racz K, Tarnok A. Quantitative histology by multicolor slide-based cytometry. *Cytometry Part A* 2004;59A(2):210-219.
9. Smolle J, Gerger A, Weger W, Kutzner H, Tronnier M. Tissue counter analysis of histologic sections of melanoma: influence of mask size and shape, feature selection, statistical methods and tissue preparation. *Anal Cell Pathol* 2002;24:59-67.
10. Tarnok A. New technologies for the Human Cytome Project. *J BRHA* 2004;18:92-95.
11. Valet G, Leary JF, Tarnok A. Cytomics - new technologies: towards a human cytome project. *Cytometry Part A* 2004;59A: 167-171.
12. Valet G. Human cytome project, cytomics, and systems biology: the incentive for new horizons in cytometry. *Cytometry Part A* 2005; 64A(1):1-2.